coatings

MDPI

Article

Surface Modification of Austenitic Stainless Steel by Means of Low Pressure Glow-Discharge Treatments with Nitrogen

Francesca Borgioli *, Emanuele Galvanetto and Tiberio Bacci

Department of Industrial Engineering, University of Florence, via S. Marta 3, 50139 Florence, Italy; emanuele.galvanetto@unifi.it (E.G.); tiberio.bacci@unifi.it (T.B.)

* Correspondence: francesca.borgioli@unifi.it; Tel.: +39-055-275-8734

Received: 26 August 2019; Accepted: 20 September 2019; Published: 24 September 2019

Abstract: When low temperature nitriding of austenitic stainless steels is carried out, it is very important to remove the surface passive layer for obtaining homogeneous incorporation of nitrogen. In the glow-discharge nitriding technique this surface activation is performed by cathodic sputtering pre-treatment, which can heat also the samples up to nitriding temperature. This preliminary study investigates the possibility of producing modified surface layers on austenitic stainless steels by performing low pressure glow-discharge treatments with nitrogen, similar to cathodic sputtering, so that surface activation, heating and nitrogen incorporation can occur in a single step having a short duration (up to about 10 min). Depending on treatment parameters, it is possible to produce different types of modified surface layers. One type, similar to that obtained with low temperature nitriding, consists mainly of S phase and it shows improved surface hardness and corrosion resistance in 5% NaCl solution in comparison with the untreated steel. Another type has large amounts of chromium nitride precipitates, which cause a marked hardness increase but a poor corrosion resistance. These surface treatments influence also water wetting properties, so that the apparent contact angle values become >90°, indicating a hydrophobic behavior.

Keywords: glow-discharge treatment; nitriding; austenitic stainless steels; AISI 202; S phase

1. Introduction

In the last few years low temperature nitriding has received increasing attention for the surface modification of austenitic stainless steels. When the treatments are performed at temperatures lower than 450 °C, the precipitation of large amounts of chromium nitrides is usually avoided and modified surface layers are produced, which consist mainly of a supersaturated interstitial solid solution of nitrogen in the expanded and distorted γ-Fe f.c.c. lattice, known as S phase or expanded austenite [1,2]. Due to this phase, having high hardness (up to 1500 HV [1]) and corrosion resistance, improvements of surface hardness, wear resistance and corrosion resistance in chloride-ion containing solutions are obtained [1,2]. Moreover, this surface modification influences also water wettability [3–5] and biocompatibility [4–6].

The characteristics of the nitrided layers depend on different nitriding techniques [1,7–10], treatment parameters [1,3,11–14] and alloy composition [1,3,11,15,16]. Even if the main critical parameter, which influences microstructure and phase composition of the modified layers, is recognized to be the treatment temperature, also treatment pressure plays a very important role. For plasma assisted nitriding techniques, treatment pressure is usually in the range 0.1–10^3 Pa, depending on the used technique. An increase of nitriding efficiency was observed decreasing the treatment pressure, and a significant nitrogen incorporation was obtained when the process was performed in the range

80–160 Pa [3,13,14,17]. Wang et al. [13] and Lu et al. [14] reported that, on AISI 304 samples, the modified layer thickness increased significantly as the treatment pressure was decreased from 400 to 100 Pa. A greater nitrogen incorporation in S phase, observed with X-ray diffraction analysis, was obtained decreasing the pressure of a 400 °C nitriding treatment from 500 to 130 Pa on both AISI 316L and AISI 202 samples [3]. Moreover, in an our previous study [17], it was shown that, using low pressures, nitride precipitation may occur also for treatment temperature and duration suitable to produce nitride-free modified layers. In fact, when nitriding treatments were carried out, on AISI 316L samples, at 430 °C for 5 h with pressures in the range 1×10^3–2×10^3 Pa, the modified surface layers consisted mainly of S phase and no nitrides were observed inside them. On the contrary, when pressures were in the range 150–500 Pa, a fairly large nitride precipitation occurred inside the modified layers, especially at grain boundaries.

In order to allow a homogeneous incorporation of nitrogen during the treatment, the passive oxide film of stainless steels has to be previously removed. This surface activation is the first and fundamental step in the nitriding treatment, and it has been shown that the pre-cleaning procedure and parameters can also influence the modified layers thickness and growth [1,18]. The cathodic sputtering technique, which is usually used as the pre-treatment of plasma nitriding or ion implantation processes, is particularly efficient [18], and it allows both surface cleaning and heating of the samples up to the treatment temperature due to ion bombardment [11]. Pre-treatments using argon [19], hydrogen [18], argon–hydrogen [20], nitrogen [18] and nitrogen–hydrogen [11] were reported, often at pressures lower than 100 Pa; the low pressures cause not only an enhancement of the sputtering effect but also a surface etching [3]. When nitrogen is used in the gas mixture, its incorporation in the surface layers may occur, depending on treatment parameters [21].

The studies on the surface activation and pre-cleaning techniques are usually focused on the efficiency of these treatments, in order to produce thicker and more homogeneous modified surface layers with the following nitriding treatment, but, to our knowledge, in the international literature a lack of information exists regarding the effects of similar plasma treatments, performed at low pressure using nitrogen, in order to produce a significant nitrogen enrichment of the surface.

This preliminary study investigates the effects of low pressure glow-discharge treatments, performed with a nitrogen containing gas mixture, on the surface modification of AISI 202 austenitic stainless steel. These treatments can be considered similar to cathodic sputtering, since they activate the surface and heat the samples, but they also allow a significant nitrogen incorporation in a fairly short duration. AISI 202 is a CrMn grade, in which nickel is partly substituted by manganese and nitrogen as austenite stabilizing elements. Even if it has a lower corrosion resistance in comparison with AISI 300 series austenitic stainless steels, when this alloy is subjected to low temperature nitriding and modified surface layers consisting mainly of the S phase are able to form, it shows a marked increase of corrosion resistance in chloride-ion containing solutions [22–24]. This steel is suitable for studying nitriding processes, since it is particularly sensitive to treatment parameters (temperature and pressure) [22–24], and it is able to form nitrides at temperatures as low as 400 °C, depending on the experimental conditions [3,23]. Microstructure, phase composition, roughness, surface microhardness, water wetting and corrosion resistance of the treated samples were studied, and they were compared with those of samples untreated and subjected to nitriding treatment.

2. Materials and Methods

Samples (40 mm × 17 mm × 0.7 mm) of AISI 202 austenitic stainless steel were obtained from cold rolled, annealed and pickled plates by cutting, grinding and polishing up to 6-μm diamond suspension. The chemical composition of the steel was (in wt.%): 0.065 C, 17.0 Cr, 4.1 Ni, 7.7 Mn, 0.40 Si and 0.15 N. X-ray diffraction analysis showed that, besides austenite, a small amount of ferrite, α-Fe (b.c.c.), was present in the steel.

Glow-discharge treatments were carried out in a laboratory plasma equipment, previously described [22]. Here we recall that the samples were fastened on a prismatic sample holder, placed in

the centre of the treatment chamber, which has an axial symmetry. The sample holder was connected to the cathode of a DC power supply and it was surrounded by a cylindrical AISI 304 screen, grounded and working as anode. The anode–cathode distance was about 60 mm. The treatment temperature was controlled varying the discharge current supplied by the power supply and it was measured by a chromel–alumel thermocouple inserted into the sample holder. Before the treatments, the treatment chamber was evacuated up to a pressure of about 5 Pa; the required treatment pressure was maintained by a flow controlled dynamic vacuum system. The experimental parameters of the low pressure treatments were chosen on the basis of our previous researches [3,16,17,22], since they allowed an activation of the surface and heating of the samples in a fairly short time with our plasma equipment configuration. The low pressure treatments were performed at 130 Pa using a 80 vol.% N_2 + 20 vol.% H_2 gas mixture in a 175 cm^3 min^{-1} (in standard conditions) flow rate. As depicted in Figure 1, the discharge current density was fixed and increased with two constant steps, while the voltage drop between the electrodes and the treatment temperature were allowed to increase freely. At the beginning the current density was fixed at 2.2 ± 0.1 mA cm^{-2}; with this condition the voltage drop between the electrodes increased from 245 ± 5 V with a rate of about 35 V min^{-1} and the treatment temperature increased from room temperature (23 °C) with a rate of about 34 °C min^{-1}. When the measured temperature reached 140 °C, current density was increased and fixed at 2.6 ± 0.1 mA cm^{-2}; with this condition the voltage drop increased with a rate changing from about 45 to about 65 V min^{-1} and the temperature with a rate of about 50 °C min^{-1}. When a prefixed voltage drop was reached, the power supply was turned off, the treatment chamber was evacuated and the samples were allowed to cool down to room temperature under vacuum. A set of samples (Type A) was treated up to a maximum voltage drop of 595 ± 5 V, reaching a measured bulk temperature of 330 °C; the duration of the treatment was 8 min. Another set (Type B) was treated up to a maximum voltage drop of 730 ± 5 V, reaching a bulk temperature of 430 °C; the duration of the treatment was 10 min. A further set of samples (Type C) was subjected to a pre-treatment with Type-A conditions (treatment up to a maximum voltage drop of 595 ± 5 V, as described above), then pressure was increased and discharge current was adjusted in order to perform nitriding at 380 °C, 500 Pa for 5 h with a treatment atmosphere of 80 vol.% N_2 and 20 vol.% H_2; during nitriding the current density was 1.6 ± 0.1 mA cm^{-2} and voltage drop 150 ± 10 V.

The microstructure of the untreated and treated samples was examined by light and scanning electron microscopies. Cross-sections were obtained by cutting the samples and mounting them with glass-filled epoxy thermosetting resin. The microstructure of the modified layers and of the matrix was delineated using acetic glyceregia etchant (3 mL HCl, 2 mL HNO_3, 2 mL acetic acid and 1 drop of glycerol).

Phases were identified using X-ray diffraction analysis (Cu Kα radiation) in Bragg-Brentano configuration (D8 Advance, Bruker AXS GmbH, Karlsruhe, Germany). A semi-quantitative evaluation of the alloy elements (Fe, Cr, Ni, Mo, Mn and Si) and of nitrogen present in the surface layers of the samples was performed by means of X-ray fluorescence (XRF; ZSX Primus II, Rigaku, Tokyo, Japan) analysis.

Roughness evaluation was carried out with a stylus profilometer, using a 2-μm radius stylus with a 1-mN contact force; the cut-off length was 0.25 mm. Ten measurements were taken at different locations on each sample. The average surface roughness R_a (arithmetical mean deviation of the roughness profile from the mean line), the maximum height of profile R_z (sum of the largest profile peak height and the largest profile valley depth within a sampling length, according to UNI EN ISO 4287:2009 norm [25]) and the mean height of profile elements R_c (mean value of the profile element heights within a sampling length) were recorded.

The apparent static contact angle of water was measured according to the sessile drop method. Bi-distilled water was employed as a test liquid, and drops of 0.5 μL were used. Before the measurement, the samples were sonicated in acetone for 5 min and then freely dried in air. For each sample the contact angle was measured at least 10 times across the sample surface. All measurements were

taken under ambient laboratory conditions. The contact angle values are given as the average value ± standard deviation.

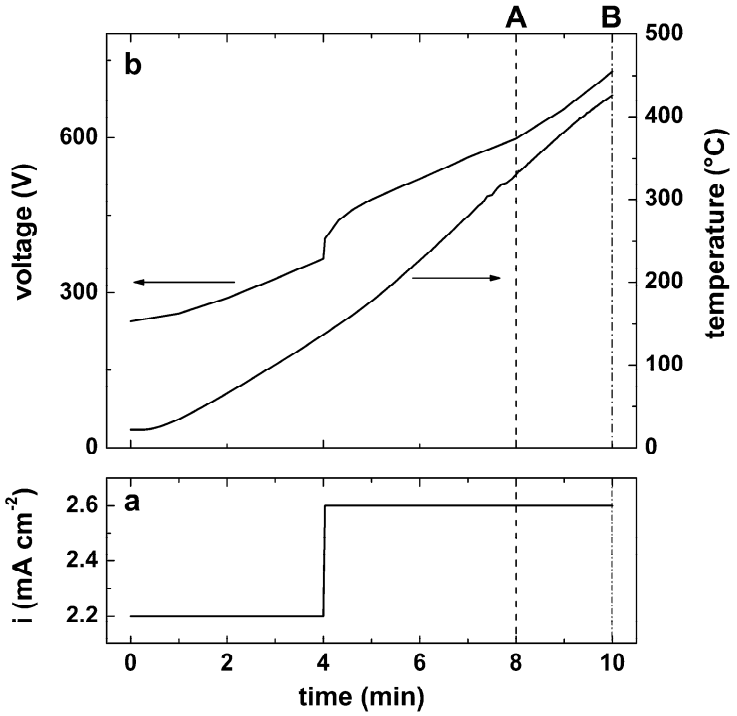

Figure 1. Current density (**a**), voltage drop and bulk temperature (**b**) as a function of time for Type-A and -B glow-discharge treatments. The vertical dashed lines, named A and B, indicate the end of Type-A and -B treatments, respectively. Type-A samples were treated up to 595 ± 5 V (treatment duration: 8 min); Type-B samples were treated up to 730 ± 5 V (treatment duration: 10 min).

Surface microhardness measurements (load: 10 and 25 gf) were carried out on the samples using a Knoop indenter.

Corrosion behavior was studied in 5% NaCl aerated solution at room temperature by means of the potentiodynamic method. Polarization tests were performed using a standard three-electrode flat cell, equipped with an Ag/AgCl reference electrode (3.5 M KCl) and a platinum grid as a counterelectrode, after a delay of 18 h and with a potential scan rate of 0.3 mV s^{-1}. The sample surface area exposed to the electrolyte was 1 cm^2. The degradation due to corrosion phenomena was evaluated also by means of coulometric analysis. Current density values of polarization curves were integrated from corrosion potential to +1000 mV (Ag/AgCl), taking into account that:

$$\text{potential (mV)/scan rate (mV s}^{-1}\text{)} = \text{time (s)}. \quad (1)$$

The integration was performed using the program Echem Analyst (Version 7.06, Gamry, Warminster, PA, USA).

3. Results

3.1. Morphology and Microstructure

After the treatment the surface of all sample types showed an etched appearance, which delineated grain boundaries with the characteristic twins. For Type-A samples, this etching, due to sputtering, was fairly low, and the grooves produced by the grinding and polishing procedure were still observable (Figure 2a). In some grains shear lines, due to local plastic deformation caused by nitrogen solubilization and the formation of modified layers, were observable. Surface roughness increased in comparison

with untreated samples (Table 1). For Type-B samples, etching was more marked, especially at grain boundaries, and roughness markedly increased (Figure 2b). When the nitriding step was also performed (Type C), the surface showed the effects of both a strong etching, due to sputtering and nitriding, and local plastic deformations, owing to the formation of modified layers (Figure 2c), and roughness increase was marked.

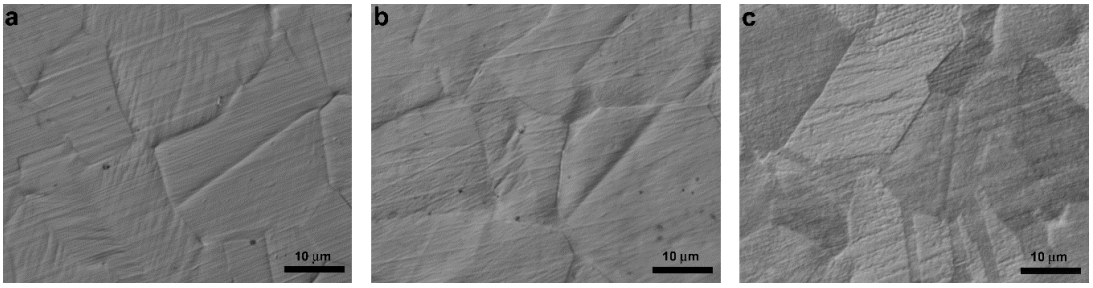

Figure 2. Surface morphology of Type-A (**a**), Type-B (**b**) and Type-C (**c**) treated samples.

Table 1. Roughness parameters R_a, R_z and R_c, for samples untreated and treated as indicated.

Sample Type	R_a (µm)	R_z (µm)	R_c (µm)
Untreated	0.007 ± 0.002	0.046 ± 0.008	0.029 ± 0.006
Type A	0.011 ± 0.002	0.09 ± 0.02	0.06 ± 0.01
Type B	0.042 ± 0.002	0.32 ± 0.04	0.20 ± 0.02
Type C	0.045 ± 0.005	0.32 ± 0.07	0.21 ± 0.05

The typical cross-section microstructure of the modified surface layers is shown in Figure 3, and X-ray diffraction patterns of untreated and treated samples are depicted in Figure 4. Type-A treatment produced modified surface layers, similar to those observed in low temperature nitrided AISI 202 stainless steel [22,24], with a thicker outer layer, in which S phase was present, and an inner layer consisting of a solid solution of interstitial atoms (nitrogen and carbon) in the slightly expanded austenite lattice, γ(N,C) (Figures 3a and 4b). The modified layers were fairly thin, had a thickness of 1.8 ± 0.2 µm as a whole. XRF analysis showed that, at the surface, a nitrogen content of about 22 at.% was present.

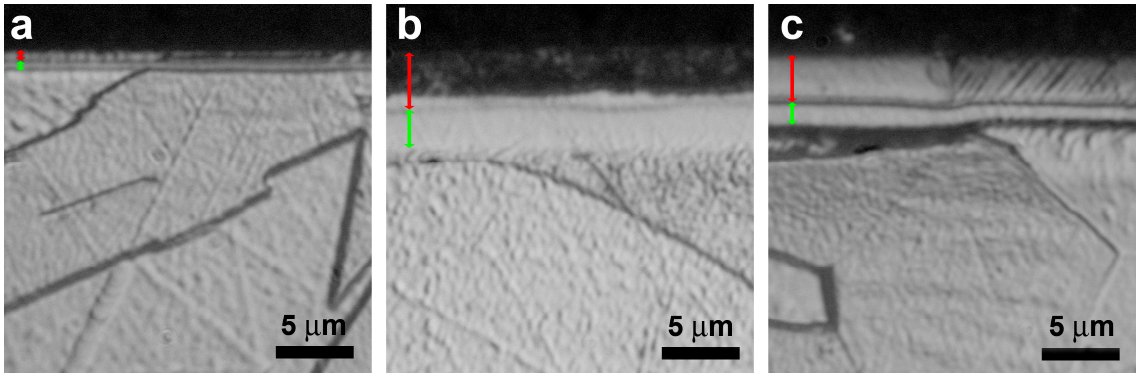

Figure 3. Micrographs of the modified surface layers of Type-A (**a**), Type-B (**b**) and Type-C (**c**) treated samples (etchant: Acetic glyceregia). The red and green markers indicate the outer and inner modified layers, respectively.

When Type-B treatment was performed, the modified layers consisted of a strongly etched outer layer and a fairly unetched inner layer (Figure 3b), having a thickness of 6.5 ± 0.3 µm as a whole. X-ray diffraction analysis showed that the phases present in the depth explored by X-ray beam were mainly CrN (f.c.c.) and α-Fe (b.c.c.) (Figure 4c); small peaks ascribable to S phase were also observed.

At the surface a nitrogen content of about 25 at.% was detected, while the average chromium, nickel and manganese content did not significantly change when compared to that of the untreated samples.

The Type-C samples had the typical double layer microstructure of low temperature nitrided AISI 202 stainless steel [22,24], with an outer surface layer, in which many thin lines, related to plastic deformation, were observable (Figure 3c). In the outer layer S phase and a solid solution of nitrogen in h.c.p. martensite, ε_N', were present, while in the inner layer γ(N,C) was detectable (Figure 4d). The modified layers had a thickness of 4.8 ± 0.3 μm as a whole. A nitrogen content of about 25 at.% was detected at the surface.

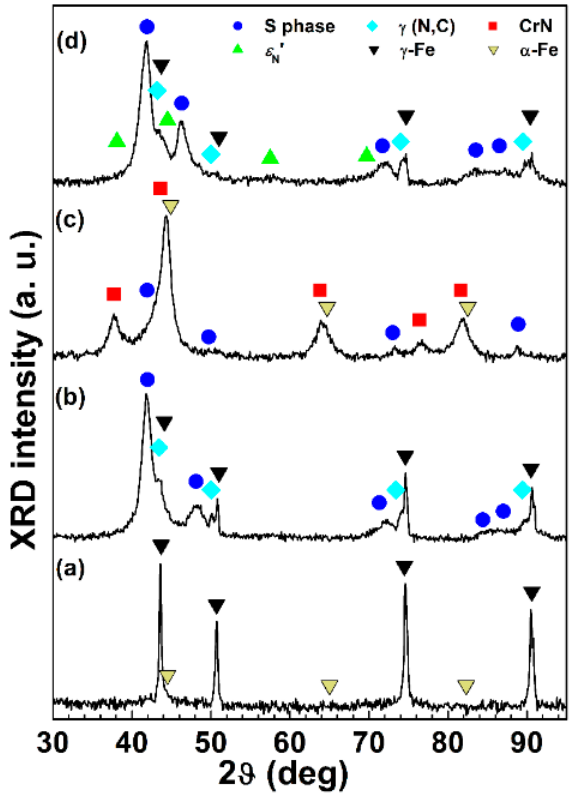

Figure 4. X-ray diffraction patterns of samples untreated (**a**) and Type-A (**b**), Type-B (**c**) and Type-C (**d**) treated.

3.2. *Water Contact Angle*

The apparent water contact angle values for untreated and treated samples are reported in Table 2. As an example, the images of drops on the surface of untreated and treated samples are shown in Figure 5. Untreated steel had hydrophilic behavior, but with a fairly large contact angle. After the treatment, for all the samples a significant increase of contact angle values was observed. For Type-A and Type-B samples the surface became hydrophobic, while for Type-C samples it remained hydrophilic, even with large contact angle values.

Table 2. Apparent contact angle (CA) for samples untreated and treated as indicated.

Sample Type	CA (°)
Untreated	73 ± 3
Type A	96 ± 2
Type B	104 ± 2
Type C	84 ± 6

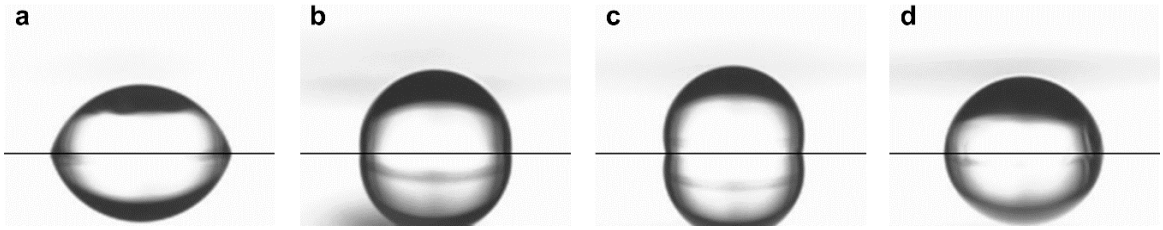

Figure 5. Images of 0.5-μL drops deposited on the surface of samples untreated (**a**), and Type-A (**b**), Type-B (**c**) and Type-C (**d**) treated. The black line is drawn as a guide to the eye to outline the surface and to separate the drop from its reflection.

3.3. Microhardness

Surface microhardness values for untreated and treated samples are reported in Table 3. As the load was increased, lower hardness values were detected, due to both the indentation size effect and the fact that layers having different characteristics were tested.

Table 3. Surface Knoop microhardness values of samples untreated and treated as indicated (test loads: 10 and 25 gf).

Sample Type	$HK_{0.01}$	$HK_{0.025}$
Untreated	339 ± 11	304 ± 5
Type A	903 ± 32	406 ± 23
Type B	1977 ± 177	1088 ± 76
Type C	1577 ± 164	795 ± 22

All the treatments were able to significantly increase the surface microhardness in comparison with the untreated alloy. Type-A samples showed only a moderate hardness increase, if compared with nitrided samples (Type C), owing to the smaller thickness of the modified layers. The hardness increase of Type-B samples was particularly marked, due to the presence of thick modified layers, which were rich in hard nitride precipitates.

3.4. Corrosion Behavior

Typical polarization curves of untreated and treated samples are shown in Figure 6.

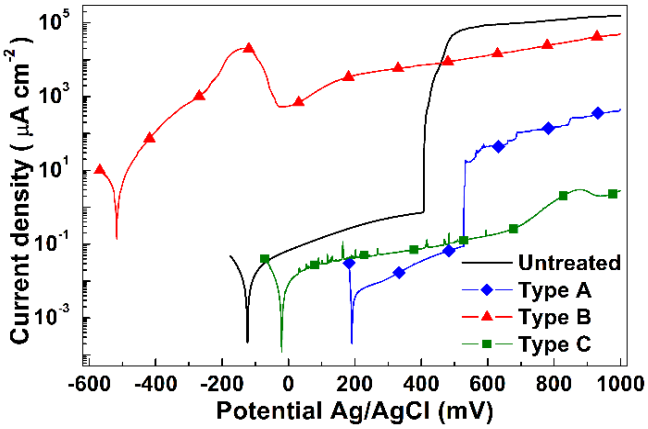

Figure 6. Polarization curves of samples untreated and treated as indicated (solution: 5% NaCl, aerated).

The untreated samples had passive corrosion behavior, with very low anodic current density values, which rapidly increased owing to the occurrence of localized corrosion phenomena when the potential was higher than about +407 mV (Ag/AgCl). After the tests the surface of the samples showed

many deep pits, randomly distributed on the surface. Crevice corrosion occurred in the area shielded by the PTFE gasket. The charge density value, obtained by integrating the anodic currents, was fairly high, $(1.9 \pm 0.1) \times 10^5$ mC cm^{-2}, indicating an extended damage.

The Type-A samples had similar passive behavior, but both corrosion and pitting potential values were significantly higher and anodic current density in the passive branch was lower, in comparison with those of untreated samples. After the tests, on the surface few shallow pits were present and a colored region was observed in correspondence to part of the gasket. The lower damage, if compared to that produced on untreated samples, was evidenced also by smaller charge density, $(2.8 \pm 0.3) \times 10^2$ mC cm^{-2}.

For Type-B samples an active corrosion behavior was registered, with a low corrosion potential and a rapid increase of anodic current density values; the charge density was $(5.6 \pm 0.2) \times 10^4$ mC cm^{-2}. After the tests, the surface of the samples was strongly colored and many deep pits were present.

The Type-C samples had the typical behavior of a low temperature nitrided austenitic stainless steel tested in NaCl solution. Corrosion potential was higher than that of the untreated steel, the passive branch was markedly wider and it had lower anodic current density. After the tests the surface of the samples showed only a small colored region corresponding to part of the gasket, while the remaining area seemed fairly untouched. The very low damage was evidenced also by the small charge density, 3 ± 1 mC cm^{-2}.

4. Discussion

The use of low pressure in glow-discharge treatments causes an increase of both the mean free path of molecules, atoms and ions present in plasma, and the discharge voltage between the electrodes. As a consequence, ion and fast neutral energy increases, so that sputtering rate becomes considerable [26] and etching is deep. The high ion energy can also increase the number of active nitrogen atoms [13,14], which are able to diffuse into the substrate if the nitrogen feeding is not completely counteracted by sputtering. Baranowska [21] and Baranowska et al. [27] reported a small nitrogen incorporation during cathodic sputtering, which can be explained taking into account the low pressure of the treatment (2–3 Pa), which causes a high sputtering rate. On the other hand, as previously recalled, it was reported that nitriding treatments performed in the range 80–160 Pa allow a significant nitrogen incorporation [3,13,14,17], suggesting that, in these conditions, nitrogen feeding is larger than sputtering.

The low pressure treatments reported in this study were performed using larger current densities and maximum voltage drop than those usually employed for nitriding [3,17], in order to have fast heating of the samples. It may be supposed that, in these conditions, not only efficient surface activation and heating of the samples can occur, but also more active nitrogen atoms are obtained, which can diffuse into the substrate and produce modified surface layers in shorter times than those usually employed in nitriding treatments.

This preliminary study points out that the used low pressure treatments are very sensitive to process parameters, so that modified surface layers having significantly different characteristics can be obtained. When lower voltage drop and temperature are attained, as for the Type-A treatment, the modified surface layers are similar to those produced by low temperature nitriding treatments having short durations (1–3 h) [24,28]. By increasing the maximum voltage drop, and thus the maximum temperature, as for the Type-B treatment, the modified surface layers are similar to those produced by nitriding at temperatures higher than 450 °C [11,22]. A large amount of CrN is able to form, and the loss of solubilized chromium from the matrix causes the subsequent transformation of f.c.c. austenite into b.c.c. α-Fe [29,30]. It is interesting to note that CrN and α-Fe formation occurs quickly, while iron based nitrides, γ'-M_4N (f.c.c.) and ε-$M_{2-3}N$ (hex.) (M = Fe, Mn, Ni, Cr) are not detected, unlike for samples nitrided at 500 °C for 5 h [22].

The increase of surface microhardness depends on the thickness of the modified layers and on the precipitation of hard nitrides, as previously reported [11,17,22,24,28], so that a small increase is observed for Type-A samples while a larger one for Type-B samples.

A fairly large nitrogen solubilization and the formation of the S phase improved the corrosion resistance of Type-A samples in NaCl solution, in comparison with the untreated steel. As previously observed [11,23,24], solubilized nitrogen has a beneficial effect, so that the corrosion potential increases and anodic current density in the passive branch decreases. For this sample type the increase of the potential, at which localized corrosion phenomena occur, was not as large as for the nitrided samples (Type C), but the level of damage was markedly lower if compared to that of untreated AISI 202, as evidenced by the coulometric analysis. This fact might be ascribed to the lower nitrogen content and smaller thickness of the modified layers, in comparison with those of the nitrided samples [23,24,31]. On the other hand, in Type-B samples the presence of CrN precipitates caused a chromium depletion in the nearby regions, so that the formation of a protective passive film was prevented and a low corrosion resistance was observed, as registered also for samples nitrided at temperatures higher than 450 °C [11,22,31,32].

For both Type-A and Type-B treatments the ion bombardment at the surface caused an etching, which was particularly marked at grain boundaries and it resulted in being stronger as the treatment was longer (Type B). Besides etching, surface morphology was affected also by the formation of modified layers, which caused local plastic deformations, as previously reported [3,11,24]. As a consequence, an increase of surface roughness was registered. The increase of the distance between peaks and valleys at the surface influences also water wettability. The increase of the apparent contact angle suggests that fakir drop lies on a composite surface of solid and air pockets trapped underneath, according to the Cassie-Baxter model [33,34]. This behavior was observed also on low temperature glow-discharge nitrided samples [3]. The combination of strong etching at grain boundaries and limited plastic deformations inside the grains seems to promote the formation of many air pockets, so that hydrophobic behavior is observed. For the nitrided samples (Type C) larger plastic deformations occurred at the surface, but the obtained results suggest that they were less efficient in producing air pockets if compared with low pressure treatments.

5. Conclusions

Modified surface layers could be produced, on AISI 202 austenitic stainless steel, by means of treatments performed with the glow-discharge technique at a pressure of 130 Pa in a 80 vol.% N_2 and 20 vol.% H_2 gas mixture, so that surface activation, heating and nitrogen incorporation can occur in a single step having a short duration (up to 10 min). Preliminary results show that the modified surface layers were very sensitive to treatment parameters. When lower voltage drop and temperature were attained, modified surface layers consisting mainly of the S phase formed, they had higher surface hardness and corrosion resistance in 5% NaCl solution than the untreated alloy. These modified layers were similar to those produced by low temperature nitriding with short treatment durations (1–3 h). On the other hand, by increasing the maximum voltage drop, and thus the maximum treatment temperature, large amounts of CrN were able to form, so that a marked increase in surface hardness and a poor corrosion resistance were observed. Both treatment conditions produced an increase of surface roughness, which affected water wetting properties, causing hydrophobic behavior.

Author Contributions: Conceptualization, F.B., E.G., T.B.; software, E.G.; formal analysis, F.B. and E.G.; investigation, F.B. and E.G.; writing—original draft preparation, F.B.; writing—review & editing, F.B. and E.G.; supervision, F.B.; project administration, F.B.; funding acquisition, F.B. and T.B.

Funding: This research was funded by MIUR (Ministero dell'Istruzione, dell'Università e della Ricerca; years 2014, 2015).

Acknowledgments: ThyssenKrupp Acciai Speciali Terni (Terni, Italy) is acknowledged for providing the AISI 202 steel.

Conflicts of Interest: The authors declare no conflict of interest.

References

1. Dong, H. S-phase surface engineering of Fe–Cr, Co–Cr and Ni–Cr alloys. *Int. Mater. Rev.* **2010**, *55*, 65–98. [CrossRef]
2. Lo, K.H.; Shek, C.H.; Lai, J.K.L. Recent developments in stainless steels. *Mater. Sci. Eng. R* **2009**, *65*, 39–104. [CrossRef]
3. Borgioli, F.; Galvanetto, E.; Bacci, T. Influence of surface morphology and roughness on water wetting properties of low temperature nitrided austenitic stainless steels. *Mater. Charact.* **2014**, *95*, 278–284. [CrossRef]
4. Buhagiar, J.; Bell, T.; Simmons, R.; Dong, H. Evaluation of the biocompatibility of S-phase layers on medical grade austenitic stainless steels. *J. Mater. Sci. Mater. Med.* **2011**, *22*, 1269–1278. [CrossRef] [PubMed]
5. Lin, Y.-H.; Lan, W.-C.; Ou, K.-L.; Liu, C.-M.; Peng, P.-W. Hemocompatibility evaluation of plasma-nitrided austenitic stainless steels at low temperature. *Surf. Coat. Technol.* **2012**, *206*, 4785–4790. [CrossRef]
6. Stio, M.; Martinesi, M.; Treves, C.; Borgioli, F. Cultures and co-cultures of human blood mononuclear cells and endothelial cells for the biocompatibility assessment of surface modified AISI 316L austenitic stainless steel. *Mater. Sci. Eng. C* **2016**, *69*, 1081–1091. [CrossRef] [PubMed]
7. Wei, R.; Vajo, J.J.; Matossian, J.N.; Wilbur, P.J.; Davis, J.A.; Williamson, D.L.; Collins, G.A. A comparative study of bean ion implantation, plasma ion implantation and nitriding of AISI 304 stainless steel. *Surf. Coat. Technol.* **1996**, *83*, 235–242. [CrossRef]
8. Czerwiec, T.; Renevier, N.; Michel, H. Low-temperature plasma assisted nitriding. *Surf. Coat. Technol.* **2000**, *131*, 267–277. [CrossRef]
9. Gallo, S.C.; Dong, H. Study of active screen plasma processing conditions for carburising and nitriding austenitic stainless steel. *Surf. Coat. Technol.* **2009**, *203*, 3669–3675. [CrossRef]
10. Borowski, T.; Adamczyk-Cieślak, B.; Brojanowska, A.; Kulikowski, K.; Wierzchoń, T. Surface modification of austenitic steel by various glow-discharge nitriding methods. *Mater. Sci.* **2015**, *21*, 376–381. [CrossRef]
11. Fossati, A.; Galvanetto, E.; Bacci, T.; Borgioli, F. Improvement of corrosion resistance of austenitic stainless steels by means of glow-discharge nitriding. *Corros. Rev.* **2011**, *29*, 209–221. [CrossRef]
12. Köster, K.; Kaestner, P.; Bräuer, G.; Hoche, H.; Troßmann, T.; Oechsner, M. Material condition tailored to plasma nitriding process for ensuring corrosion and wear resistance of austenitic stainless steel. *Surf. Coat. Technol.* **2013**, *28*, S615–S618. [CrossRef]
13. Wang, S.; Cai, W.; Li, J.; Wei, W.; Hu, J. A novel rapid D.C. plasma nitriding at low gas pressure for 304 austenitic stainless steel. *Mater. Lett.* **2013**, *105*, 47–49. [CrossRef]
14. Lu, S.; Zhao, X.; Wang, S.; Li, J.; Wei, W.; Hu, J. Performance enhancement by plasma nitriding at low gas pressure for 304 austenitic stainless steel. *Vacuum* **2017**, *145*, 334–339. [CrossRef]
15. Egawa, M.; Ueda, N.; Nakata, K.; Tsujikawa, M.; Tanaka, M. Effect of additive alloying element on plasma nitriding and carburizing behavior for austenitic stainless steels. *Surf. Coat. Technol.* **2010**, *205*, S246–S251. [CrossRef]
16. Borgioli, F.; Galvanetto, E.; Bacci, T. Low temperature nitriding of AISI 300 and 200 series austenitic stainless steels. *Vacuum* **2016**, *127*, 51–60. [CrossRef]
17. Borgioli, F.; Fossati, A.; Galvanetto, E.; Bacci, T.; Pradelli, G. Glow discharge nitriding of AISI 316L austenitic stainless steel: Influence of treatment pressure. *Surf. Coat. Technol.* **2006**, *200*, 5505–5513. [CrossRef]
18. Baranowska, J. Importance of surface activation for nitrided layer formation on austenitic stainless steel. *Surf. Eng.* **2010**, *26*, 293–298. [CrossRef]
19. Abrasonis, G.; Rivière, J.P.; Templier, C.; Muzard, S.; Pranevicius, L. Influence of surface preparation and ion flux on the nitriding efficiency of austenitic stainless steel. *Surf. Coat. Technol.* **2005**, *196*, 279–283. [CrossRef]
20. Czerwiec, T.; He, H.; Weber, S.; Dong, C.; Michel, H. On the occurrence of dual diffusion layers during plasma-assisted nitriding of austenitic stainless steel. *Surf. Coat. Technol.* **2006**, *200*, 5289–5295. [CrossRef]
21. Baranowska, J. Characteristic of the nitride layers on the stainless steel at low temperature. *Surf. Coat. Technol.* **2004**, *180–181*, 145–149. [CrossRef]
22. Borgioli, F.; Fossati, A.; Matassini, G.; Galvanetto, E.; Bacci, T. Low temperature glow-discharge nitriding of a low nickel austenitic stainless steel. *Surf. Coat. Technol.* **2010**, *204*, 3410–3417. [CrossRef]
23. Borgioli, F.; Fossati, A.; Raugei, L.; Galvanetto, E.; Bacci, T. Low temperature glow-discharge nitriding of stainless steels. In Proceedings of the 7th European Stainless Steel Conference—Science and Market, Como, Italy, 21–23 September 2011.

24. Borgioli, F.; Galvanetto, E.; Bacci, T. Corrosion behaviour of low temperature nitrided nickel-free, AISI 200 and AISI 300 series austenitic stainless steels in NaCl solution. *Corros. Sci.* **2018**, *136*, 352–365. [CrossRef]
25. UNI EN ISO 4287:2009. *Geometrical Product Specifications (GPS)—Surface Texture: Profile Method—Terms, Definitions and Surface Texture Parameters*; UNI—Italian Organization for Standardization: Milan, Italy, 2009.
26. Ruset, C.; Ciuca, S.; Grigore, E. The influence of the sputtering process on the constitution of the compound layers obtained by plasma nitriding. *Surf. Coat. Technol.* **2003**, *174–175*, 1201–1205. [CrossRef]
27. Baranowska, J.; Kusior, E.; Amigo, V.; Szczeciński, K. Surface modification of austenitic steel by low-temperature plasma. *Vacuum* **2005**, *78*, 389–394. [CrossRef]
28. Fossati, A.; Borgioli, F.; Galvanetto, E.; Bacci, T. Glow-discharge nitriding of AISI 316L austenitic stainless steel: Influence of treatment time. *Surf. Coat. Technol.* **2006**, *200*, 3511–3517. [CrossRef]
29. Collins, G.A.; Hutchings, R.; Short, K.T.; Tendys, J.; Li, X.; Samandi, M. Nitriding of austenitic stainless steel by plasma immersion ion implantation. *Surf. Coat. Technol.* **1995**, *74–75*, 417–424. [CrossRef]
30. Menthe, E.; Rie, K.-T. Further investigation of the structure and properties of austenitic stainless steel after plasma nitriding. *Surf. Coat. Technol.* **1999**, *116–119*, 199–204. [CrossRef]
31. Fossati, A.; Borgioli, F.; Galvanetto, E.; Bacci, T. Corrosion resistance properties of glow-discharge nitrided AISI 316L austenitic stainless steel in NaCl solutions. *Corros. Sci.* **2006**, *48*, 1513–1527. [CrossRef]
32. Bell, T. Surface engineering of austenitic stainless steel. *Surf. Eng.* **2002**, *18*, 415–422. [CrossRef]
33. Cassie, A.B.D.; Baxter, S. Wettability of porous surfaces. *Trans. Faraday Soc.* **1944**, *40*, 546–550. [CrossRef]
34. Quéré, D. Wetting and roughness. *Ann. Rev. Mater. Res.* **2008**, *38*, 71–99. [CrossRef]